



Electron dynamics in nanoscale transistors by means of Wigner and Boltzmann approaches

J.M. Sellier^{a,*}, S.M. Amoroso^b, M. Nedjalkov^c, S. Selberherr^c, A. Asenov^{b,d}, I. Dimov^a

^a IICT, Bulgarian Academy of Sciences, Acad. G. Bontchev str. Bl25A, 1113 Sofia, Bulgaria

^b University of Glasgow, G12 8LT Glasgow, UK

^c Institute for Microelectronics, TU Wien, Gußhausstraße 27–29/E360, 1040 Wien, Austria

^d Gold Standard Simulation Ltd., G12 8QQ Glasgow, UK

HIGHLIGHTS

- We use the two-dimensional, time-dependent, Wigner MC method.
- We simulate the evolution of a Gaussian wave packet moving in a realistic channel potential.
- We include the kernel of a scattering center in the channel.
- We compare the Wigner results with the Boltzmann results.

ARTICLE INFO

Article history:

Received 26 September 2013

Received in revised form 3 December 2013

Available online 28 December 2013

Keywords:

Full quantum transport
Wigner equation
Boltzmann equation
Monte Carlo methods
Nanometer scaled devices
Single dopants

ABSTRACT

We present a numerical study of the evolution of a wave packet in a nanoscale MOSFET featuring an ‘atomistic’ channel doping. Our two-dimensional Monte Carlo Wigner simulation results are compared against classical Boltzmann simulation results. We show that the quantum effects due to the presence of a scattering center are manifestly non-local affecting the wave propagation much farther than the geometric limit of the center. In particular the part of the channel close to the oxide interface remains blocked for transport, in contrast to the behavior predicted by classical Boltzmann propagation.

© 2013 Elsevier B.V. All rights reserved.

1. Introduction

With shrinking transistors dimensions down to nanometric size, the device electrical behavior starts to be dominated by both the granularity of matter [1–10] and quantum mechanical effects [11,12]. In order to preserve accuracy and reliability at the nanoscale regime, device simulation approaches have, on one hand, to depart from treating the doping as a continuum, within the Poisson equation only, and, on the other hand, to improve the traditional semi-classical modeling of transport to properly take into account the particle–wave duality. The particle-based Wigner Monte Carlo (MC) approach has been recently shown to efficiently deal with the simulation of full quantum transport [13]. In particular a Wigner MC method, based on particle’s sign, for stationary cases [14] has been recently generalized for time-dependent simulations [15]. This method is general enough to deal with multi-dimensional domains. In this work we apply it to simulate two-dimensional

* Corresponding author. Tel.: +359 029796619.

E-mail address: jeanmichel.sellier@gmail.com (J.M. Sellier).

electron evolution in the channel of a nanoscale MOSFET in the presence of a single discrete dopant. The evolution problem is posed by an initial condition, there are no injecting boundaries as in the stationary problems posed by boundary conditions [16].

Our simulation results are, first of all, validated against two one-dimensional (1D) benchmarks based on the ballistic Boltzmann equation for the case of a constant applied electric field and the solution of the Schrödinger equation for the case of an idealistic potential barrier. Then, two-dimensional (2D) full quantum results are compared with results of the classical Boltzmann MC approach for a realistic device potential. Due to the non-local quantum effects, the discrete scattering center affects the wave propagation even when not directly interacting with it, blocking the charge propagation in the region close to the channel interface. These results are manifestly in contrast with the behavior predicted by classical Boltzmann propagation and demonstrate the importance of full quantum approaches for studying the electron dynamics in nanoscale devices.

2. Numerical methodology

In order to obtain a realistic potential profile of a nanoscale device, we have performed three-dimensional (3D) TCAD simulations of a well-scaled 25 nm MOSFET device using the GSS ‘atomistic’ simulator GARAND [17]. A vertical slice of the 3D device is then extracted and used to perform a 2D Wigner simulation of the charge transport in the presence of a discrete dopant. For the sake of simplicity, we account for the long range Coulombic nature of the impurity, calculated by a self-consistent Drift–Diffusion simulation, and focus on the internal kernel modeled by a rectangular potential barrier.

Concerning the quantum transport, the GNU package Archimedes [18] has been enhanced to implement the Wigner MC method, as formulated below for an initial condition. The method can actually be included in every MC platform, since it does not depend on the particular instance of the implementation. The model, a reformulation of the density matrix formalism, reads

$$\frac{\partial f_W}{\partial t} + \frac{1}{\hbar} \nabla_{\mathbf{k}} \epsilon(\mathbf{k}) \cdot \nabla_{\mathbf{x}} f_W = Q[f_W] \quad (1)$$

where $Q[f]$ is a quasi-distribution functional defined as

$$Q[f_W](\mathbf{x}, \mathbf{k}, t) = \int d\mathbf{k}' V_W(\mathbf{x}, \mathbf{k} - \mathbf{k}', t) f_W(\mathbf{x}, \mathbf{k}', t). \quad (2)$$

The function $V_W = V_W(\mathbf{x}, \mathbf{k}, t)$, known as the Wigner potential, is defined as

$$V_W(\mathbf{x}, \mathbf{k}, t) = \frac{1}{i\hbar(2\pi)^d} \int d\mathbf{x}' e^{-i\mathbf{k}\cdot\mathbf{x}'} \left(V\left(\mathbf{x} + \frac{\mathbf{x}'}{2}, t\right) - V\left(\mathbf{x} - \frac{\mathbf{x}'}{2}, t\right) \right) \quad (3)$$

where $d = 1, 2, 3$ is the dimensionality of the problem; $V = V(\mathbf{x}, t)$ is a potential defined over the spatial domain and can be time dependent.

The Monte Carlo technique exploits the semi-discrete nature of the phase-space in accordance to the principles of quantum mechanics [15]. The main purpose of this method is to evaluate an expectation value $\langle A \rangle(t)$, expressed as an iterative series, of a macroscopic physical quantity $A = A(\mathbf{x}, \mathbf{k})$, defined over the Wigner phase-space

$$\langle A \rangle = \int_0^\infty dt' \int d\mathbf{x}_i \sum_{\mathbf{m}'=-\infty}^{\infty} f_i(\mathbf{x}_i, \mathbf{m}') e^{-\int_0^{t'} \gamma(\mathbf{x}_i(y)) dy} g(\mathbf{x}_i(t'), \mathbf{m}', t') \quad (4)$$

with

$$\mathbf{x}'(y) = \mathbf{x}_i(y) = \mathbf{x}_i + \frac{\hbar \mathbf{m}' \Delta \mathbf{k}}{m^*} y; \quad \mathbf{x}' = \mathbf{x}'(t') = \mathbf{x}_i(t'); \quad d\mathbf{x}' = d\mathbf{x}_i.$$

The functions $f_i = f_i(\mathbf{x}, \mathbf{m})$ and $g = g(\mathbf{x}(t), \mathbf{m}, t)$ are, respectively, the initial quasi-distribution function and the solution of the adjoint equation [14], the kernel of which reads

$$\Gamma(\mathbf{x}, \mathbf{m}, \mathbf{m}') = V_w^+(\mathbf{x}, \mathbf{m} - \mathbf{m}') - V_w^+(\mathbf{x}, -(\mathbf{m} - \mathbf{m}')) + \gamma(\mathbf{x}) \delta_{\mathbf{m}, \mathbf{m}'}. \quad (5)$$

Finally, the quantity $\gamma(\mathbf{x})$ is defined as

$$\gamma(\mathbf{x}) = \sum_{\mathbf{m}=-\infty}^{\infty} V_w^+(\mathbf{x}, \mathbf{m}), \quad (6)$$

where V_w^+ takes the values of V_w if $V_w > 0$ and 0 otherwise.

Then the estimator of the expectation value (which can be considered also as a functional of the solution) can be expressed as weights of values of V_w at points taken in accordance with the transition probabilities. Details of the algorithm are given in Ref. [19] as well as in Ref. [20]. We also do not consider the problem of convergency. The analysis of convergency is

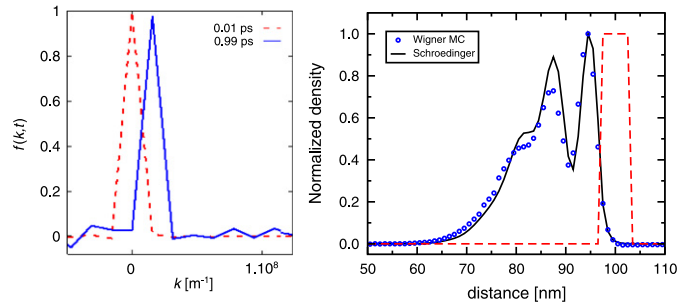


Fig. 1. Left: at times corresponding to Newton's law, the peaks not only reappear but also the nonphysical oscillations are dampened to a minimum. Right: comparison of Wigner and Schrödinger evolution of a Gaussian wave packet interacting with a 1D potential barrier at 30 fs. The barrier is shown in normalized scale (dashed line) with a thickness of 6 nm and a height of 0.3 eV.

similar to the analysis of Neumann series convergence proved in Section 10.3.3 of Ref. [19] for the Levinson and Barker–Ferry equations. The approach used in our study is based on the iterative Monte Carlo method for integral operators and has an optimal rate of convergence with reduced variance. For more details, see Ref. [19].

However, a physical interpretation of (5) can be given. If we consider the quantity $\gamma = \gamma(\mathbf{x})$ as a normalization factor, (5) describes a generation process, where an initial particle provided with a sign (represented by the δ function) creates a pair of particles, one with a positive and the other with a negative sign. In other words, if an initial particle with sign s and wave-vector \mathbf{n} generates, with a rate $V^+(\mathbf{l})$, a pair of particles with signs $s, -s$ and momenta $\mathbf{n}' = \mathbf{n} + \mathbf{l}, \mathbf{n}'' = \mathbf{n} - \mathbf{l}$, it continues its free flight evolution until a given time T .

One final note about this method must be given. In contrast to classical particles driven by the first derivative of the electric potential, quantum particles feel all other derivatives, as can be shown by the Taylor series expansion of the Wigner potential [14,15,21]. This is a manifestation of the non-locality of the quantum electron-potential interaction. Instead of a classical acceleration over Newton trajectories by the local field inherent for the device Monte Carlo approach, the action of the Wigner potential on the quantum particles representing a single electron is by generation of particles with opposite sign, locally in the position and following certain rules in the momentum component of the phase space. Thus signed particles evolve over field-less Newton trajectories and contribute to the values of the physical averages by their sign. The time-dependent evolution of the Wigner quasi-distribution happens only by creation and annihilation of particles which replace the acceleration due to Newtonian forces [15].

3. Simulation results

We started our analysis validating our full quantum Wigner MC approach against two benchmark models based on the Boltzmann and the Schrödinger equations [13,15,22,23]. We would like to emphasize that the Wigner MC method is intrinsically three-dimensional so that the validation process makes sense independent of the dimensionality of the selected benchmark test. For the sake of simplicity we report the validation results against 1D problems. In the first case an initial δ -function is defined in the phase-space with a constant electric field. Asymptotically, the Wigner solution must be equal to the Boltzmann one and must correspond to a peak moving in the phase-space at a constant pace [15]. The left plot of Fig. 1 shows the time dependent evolution of the peak at 0.01 and 0.99 ps respectively. Note that the ballistic Boltzmann solution corresponding to Newtonian acceleration is completely reconstructed only by an annihilation–creation process. In the second case an idealized 1D square barrier is used as a benchmark test. The barrier is in the middle of a 200 nm domain and has a 6 nm thickness and is 0.3 eV high. A Gaussian wave packet is evolved in time with both Wigner and Schrödinger approaches until 30 fs. As shown in the right plot of Fig. 1, there is good agreement despite the fact that the two numerical methods are very different—indeed the approach based on the Wigner equation is a MC-based method while the Schrödinger equation is solved by an implicit finite difference method [23].

Fig. 2 (left) shows the Wigner simulation results for the evolution of a 2D Gaussian wave packet:

$$f_W^0(\mathbf{x}, \mathbf{m}) = N e^{-\frac{(\mathbf{x}-\mathbf{x}_0)^2}{\sigma^2}} e^{-(\mathbf{m}\Delta\mathbf{k}-\mathbf{k}_0)^2\sigma^2}, \quad (7)$$

representing the initial electron quantum state, where $N, \mathbf{k}_0, \mathbf{x}_0$, and σ are a constant of normalization, the initial wave vector, the initial position, and the width of the wave packet. Its initial position is close to the barrier with an initial energy of 0.15 eV and an initial velocity oblique to the direction of the silicon oxide interface. The value of σ is 1 nm. A high barrier is placed at the interface between the channel and the oxide with an energy of 1.5 eV so that the packet can eventually tunnel towards the gate contact. The scattering barrier given by the discrete dopant is approximated by a 2D square barrier with energy 0.5 eV and width 0.3 nm and distance 0.4 nm from the oxide interface. This impurity potential together with the channel potential give rise to the Wigner potential (3) responsible for the evolution of the wave packet. Indeed, one can observe that the wave packet starts to interact with the scattering center before entering directly in contact with it (middle plot). This is a typical phenomenon of a quantum regime. Eventually, the initial superposition of pure states is dephased

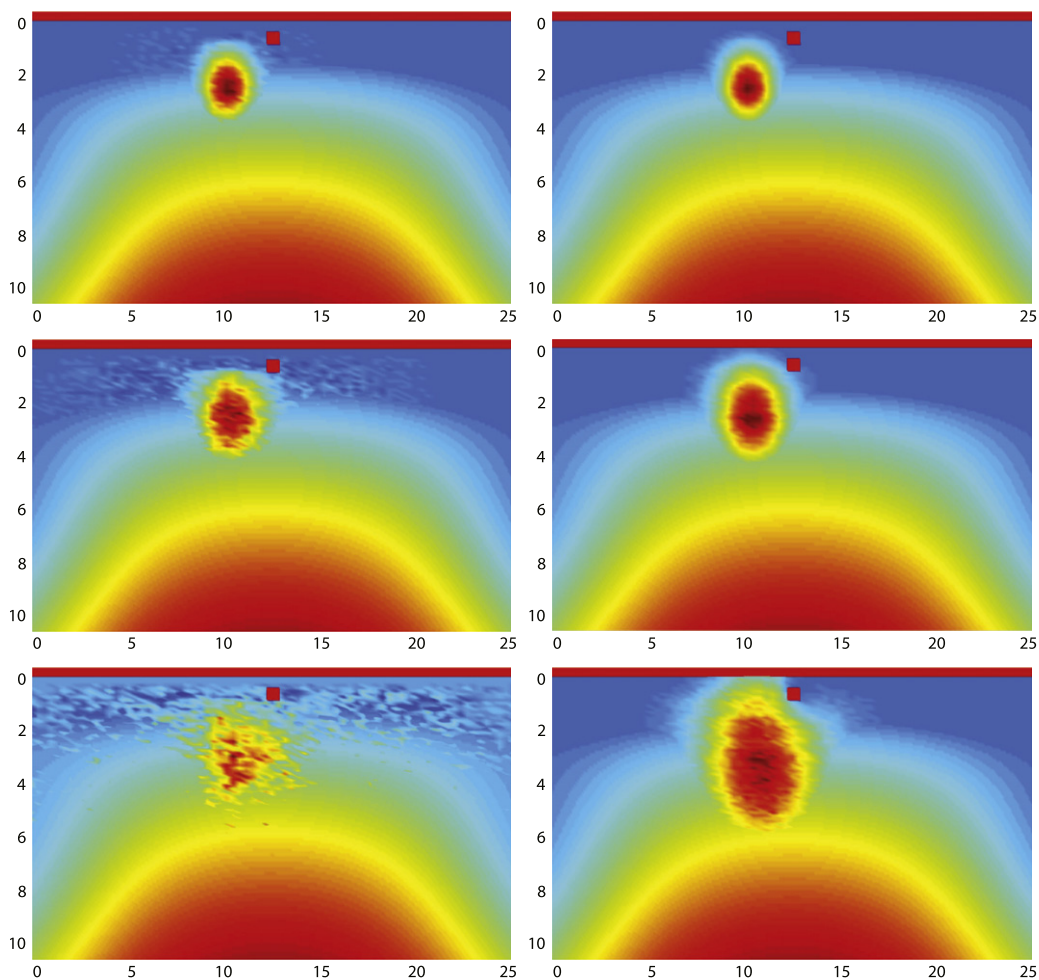


Fig. 2. Full-quantum Wigner (left) and classical Boltzmann (right) evolution of a 2D Gaussian wave packet in a 25 nm MOSFET in the presence of a discrete dopant in the channel. The electron dynamics is shown at 2 fs (top), 4 fs (middle), and 8 fs (bottom). The colormap corresponds to arbitrary units (red is high, blue is low). (For interpretation of the references to colour in this figure legend, the reader is referred to the web version of this article.)

(bottom plot) and the packet scatters back. Due to the non-locality one also observes that the wave packet never reaches the oxide. In fact, note that in the bottom plot, which corresponds to 8 fs evolution, the packet becomes local (narrower peak) and it is already bouncing back.

Furthermore, Fig. 2 (right) shows the Boltzmann simulation results in the same situation and at the same times as the ones reported for the Wigner MC method. The dynamics is classical, here the wave packet is interpreted as an initial statistical distribution. For this simulation non-local effects are absent: those electrons from the packet, which have energies below the barrier height are directly scattered from the surface of the scattering center. Indeed, the spread of the packet is more pronounced with respect to the Wigner dynamics and, eventually, the charge reaches the oxide barrier totally surrounding the scattering center. In particular, one observes a current flow between the oxide and the scattering center in contrast to the full-quantum evolution.

Classical MC simulation results reported in Refs. [24,25] have identified the scattering due to discrete dopants in the channel as an additional source of drain current variability to be taken into account with respect to the only random dopant-induced electrostatic potential fluctuations. Our results show that these effects are amplified by the non-locality affecting the charge carriers dynamics through the channel, when transport is not in a classical regime.

4. Conclusions

We have studied the evolution of a wave packet in a nanoscale MOSFET featuring discrete channel dopants. Our 2D MC Wigner simulation approach is able to capture both the quantum and the transient nature of charge carrier dynamics in the presence of scattering centers. In particular, the scattering process is strongly non-local due the quantum effects dominating the packet evolution in the nanometric domain. Contrary to what predicted by classical Boltzmann evolution, the propagation of carriers is dramatically suppressed in the part of the channel between the scattering center and the

interface, when the full-quantum Wigner formalism is adopted. These non-local scattering effects on transport give an additional contribution to the drain current variability with respect to what is captured in classical MC simulations.

Acknowledgment

The research activity leading to this work has been partially supported by the EC through the FP7 project no. 261868 MORDRED, the FP7 project AComIn (FP7 REGPOT-2012-2013-1), and the FP7 project no. 318458 SUPERTHEME.

References

- [1] R.W. Keyes, Effect of randomness in the distribution of impurity ions on FET thresholds in integrated electronics, *IEEE J. Solid-State Circuits* 4 (1975) 245–247.
- [2] P.A. Stolk, D.B.M. Klaassen, The effect of statistical dopant fluctuations on MOS device performance, *IEDM Tech. Dig.* (1996) 627–630.
- [3] D.J. Frank, R.H. Dennard, E. Nowak, P.M. Solomon, Y. Taur, H.-S.P. Wong, Device scaling limits of Si MOSFETs and their application dependencies, *Proc. IEEE* 89 (2001) 259–288.
- [4] A. Asenov, A.R. Brown, J.H. Davies, S. Kaya, G. Slavcheva, Simulation of intrinsic parameter fluctuations in decanometre and nanometre scale MOSFETs, *IEEE Trans. Electron Devices* 50 (2003) 1837–1852.
- [5] T. Shinada, S. Okamoto, T. Kobayashi, I. Ohdomari, Enhancing semiconductor device performance using ordered dopant arrays, *Nature* 437 (2005) 1128–1131.
- [6] K. Sonoda, K. Ishikawa, T. Eimori, O. Tsuchiya, Discrete dopant effects on statistical variation of random telegraph signal magnitude, *IEEE Trans. Electron Devices* 54 (2007) 1918–1925.
- [7] H. Dadgour, K. Endo, K. Banerjee, Modeling and analysis of grain-orientation effects in emerging metal-gate devices and implications for SRAM reliability, *IEDM, Tech. Dig.* (2008) 705–708.
- [8] G. Roy, A.R. Brown, F. Adamu-Lema, S. Roy, A. Asenov, Simulation study of individual and combined sources of intrinsic parameter fluctuations in conventional nano-MOSFETs, *IEEE Trans. Electron Devices* 53 (2006) 3063–3069.
- [9] A.R. Brown, N.M. Idris, J.R. Watling, A. Asenov, Impact of metal gate granularity on threshold voltage variability: a full-scale three-dimensional statistical simulation study, *IEEE Electron Device Lett.* 31 (2010) 1199–1201.
- [10] P.M. Koenraad, M.E. Flatte, Single dopants in semiconductors, *Nature Mater.* 10 (2011) 91–100.
- [11] A. Asenov, G. Slavcheva, A.R. Brown, J.H. Davies, S. Saini, Increase in the random dopant induced threshold fluctuations and lowering in sub-100 nm MOSFETs due to quantum effects: a 3-D density-gradient simulation study, *IEEE Trans. Electron Devices* 48 (2001) 722–729.
- [12] M. Luisier, A. Schenk, W. Fichtner, Quantum transport in two- and three-dimensional nanoscale transistors: coupled mode effects in the nonequilibrium Green's function formalism, *J. Appl. Phys.* 100 (2006) 043713.
- [13] D. Querlioz, P. Dollfus, *The Wigner Monte Carlo Method for Nanoelectronic Devices—A Particle Description of Quantum Transport and Decoherence*, ISTE-Wiley, 2010.
- [14] M. Nedjalkov, H. Kosina, S. Selberherr, Ch. Ringhofer, D.K. Ferry, Unified particle approach to Wigner–Boltzmann transport in small semiconductor devices, *Phys. Rev. B* 70 (2004) 115319–115335.
- [15] M. Nedjalkov, P. Schwaha, S. Selberherr, J.M. Sellier, D. Vasileska, Wigner quasi-particle attributes: an asymptotic perspective, *Appl. Phys. Lett.* 102 (2013) 163113.
- [16] R. Rosati, F. Dolcini, R.C. Iotti, F. Rossi, Wigner-function formalism applied to semiconductor quantum devices: failure of the conventional boundary condition scheme, *Phys. Rev. B* 88 (2013) 035401.
- [17] www.goldstandardsimulations.com.
- [18] www.gnu.org/software/archimedes, www.nano-archimedes.com.
- [19] I. Dimov, *Monte Carlo Methods for Applied Scientists*, World Scientific, New Jersey, London, 2008, p. 291. ISBN: 13 978-981-02-2329-8, 10 981-02-2329-3.
- [20] M. Nedjalkov, D. Vasileska, I.T. Dimov, G. Arsov, Mixed initial–boundary value problem in particle modeling of microelectronic devices, *Monte Carlo Methods Appl.* 13 (4) (2007) 299–331.
- [21] C. Jacoboni, L. Reggiani, The Monte Carlo method for the solution of charge transport in semiconductors with applications to covalent materials, *Rev. Modern Phys.* 55 (1983) 655–705.
- [22] L. Shifren, D.K. Ferry, Particle Monte Carlo simulation of wigner function tunneling, *Phys. Lett. A* 285 (2001) 217–221.
- [23] A. Goldberg, H.M. Schey, Computer-generated motion pictures of one-dimensional quantum-mechanical transmission and reflection phenomena, *Amer. J. Phys.* 35 (1967) 177–186.
- [24] C. Alexander, A.R. Brown, J.R. Watling, A. Asenov, Impact of scattering in atomistic device simulations, *Solid-State Electron.* (2005) 733–739.
- [25] C. Alexander, G. Roy, A. Asenov, Random-dopant-induced drain current variation in nano-MOSFETs: a three-dimensional self-consistent Monte Carlo simulation study using 'ab initio' ionized impurity scattering, *IEEE Trans. Electron Devices* (2008) 3251–3258.